Selection rules for nuclear spin modifications in ion-neutral reactions involving H_3^+

M. Cordonnier,[a] D. Uy,[b] R. M. Dickson,[c] K. E. Kerr,[d] Y. Zhang,[e] and T. Oka[f]
Department of Chemistry, Department of Astronomy and Astrophysics, and the Enrico Fermi Institute, The University of Chicago, Chicago, Illinois 60637

(Received 29 November 1999; accepted 4 February 2000)

We present experimental evidence for nuclear spin selection rules in chemical reactions that have been theoretically anticipated by Quack [M. Quack, Mol. Phys. **34**, 477 (1997)]. The abundance ratio of *ortho*-H_3^+ ($I=3/2$) and *para*-H_3^+ ($I=1/2$), $R=[o\text{-}H_3^+]/[p\text{-}H_3^+]$, has been measured from relative intensities of their infrared spectral lines in hydrogen plasmas using *para*-H_2 and normal-H_2 (75% o-H_2 and 25% p-H_2). The observed clear differences in the value of R between the p-H_2 and n-H_2 plasmas demonstrate the spin memory of protons even after ion-neutral reactions, and thus the existence of selection rules for spin modifications. Both positive column discharges and hollow cathode discharges have been used to demonstrate the effect. Experiments using pulsed plasmas have been conducted in the hollow cathode to minimize the uncertainty due to long-term conversion between p-H_2 and o-H_2 and to study the time dependence of the o-H_3^+ to p-H_3^+ ratio. The observed $R(t)$ has been analyzed using simultaneous rate equations assuming the nuclear spin branching ratios calculated from Quack's theory. In p-H_2 plasmas, the electron impact ionization followed by the ion-neutral reaction $H_2^+ + H_2 \rightarrow H_3^+ + H$ produces pure p-H_3^+, but the subsequent reaction between p-H_3^+ and p-H_2 scrambles protons. While the proton hop reaction (rate constant k_H) maintains the purity of p-H_3^+, the hydrogen exchange reaction (rate constant k_E) produces o-H_3^+ and acts as the gateway for nuclear spin conversion. The value of $R(t)$, therefore, depends critically on the ratio of their reaction rates $\alpha = k_H/k_E$. From observed values of $R(t)$, the ratio has been determined to be $\alpha = 2.4$. This is in approximate agreement with the value reported by Gerlich using isotopic species.
 [S0021-9606(00)01016-3]

I. INTRODUCTION

Selection rules observed in various physical and chemical processes, the rules that give the relationship between sets of quantum numbers before and after such interactions, are fascinating phenomena revealing both the symmetry and the order of magnitude of the interaction. The quantum numbers specifying the molecular states under consideration such as the rotational angular momentum, the parity, and the nuclear spin modification, result from the symmetry (or invariance) of the Hamiltonian of the free molecule with respect to rotation, space inversion, and the permutation of identical nuclei.[1] Therefore, selection rules depend on how such symmetry is broken by the interaction, and the rigor with which the selection rules are followed depends on the weakness of the interaction. If the order of magnitude of interaction energy is much smaller than that of the energy spacing of eigenstates, the interaction can be treated by perturbation theory with good convergence leading to well-obeyed selection rules.

It is well-known that radiative processes, spectroscopy, obey the simplest selection rules most rigorously.[2] This is because of the homogeneity of the interaction μE and its smallness ($\mu E/h \lesssim 1$ MHz). Only when monochromatic radiation with high-power density is applied do multiphoton processes become significant. Collisional processes, on the other hand, involve more inhomogeneous higher multipole interactions and have higher interaction energies on the order of $kT \sim 200\ \mathrm{cm}^{-1}$ at room temperature. These together lead to a more relaxed set of approximate selection rules for the angular momentum and parity.[3]

For both radiative and collisional processes, however, experiments have shown that the selection rules on the conservation of nuclear spin modifications, $\Delta I = 0$, hold most rigorously.[2,3] The spin modifications are specified by the total nuclear spin quantum number corresponding to $\underset{\sim}{I} = \Sigma_i \underset{\sim}{I}_i$ where i runs over equivalent nuclei. The I quantum number specifies the symmetry of the nuclear spin state with respect to the permutation of identical nuclei. Thus, $I=1$ and $I=0$ for *ortho* (A) and *para* (B) H_2, $I=3/2$ and 1/2 for *ortho* (A') and *para* (E') NH_3, and $I=1$, 2, and 0 for *ortho* (F_2), *meta* (A_1), and *para* (E) CH_4.[4] The robustness of the $\Delta I = 0$ rule in those molecules is due to the smallness of the inhomogeneous nuclear spin interaction ($\sim$1 kHz) compared to the

[a]Present address: Laboratoire de Physique des Lasers, Atomes et Molécules (PhLAM), Associé au CNRS, UMR 8523, Université des Sciences et Technologies de Lille, Villeneuve d'Ascq, F-59655-France.
[b]Present address: Physics Dept., Ford Motor Company, PO Box 2053, MD 3028/SRL, Dearborn, MI 48121.
[c]Present address: Department of Chemistry and Biochemistry, Georgia Institute of Technology, Atlanta, GA 30332-0400.
[d]Present address: ARCH Venture Partners, Chicago, IL 60603.
[e]Present address: Xerox Corporation, 200 Crosskeys Office Park, Fairport, NY 14450.
[f]Electronic mail: t-oka@uchicago.edu

separation of their rotational levels.[5] Spin statistics requires that nuclear spin states with certain symmetry have to be combined with rotational states such that the total wave function remains invariant other than changing its sign when two fermions are interchanged. The only clear examples where this rule is violated in radiative[6,7] or collisional[8] interactions are the cases where rotational levels with different symmetries are brought closer by an applied magnetic[6] or electric[8] field or in the heavy spherical top where rotational levels are extremely close.[7] The reluctance of nuclear spins to reorient even under strong intermolecular interaction forms the basis of the motional narrowing in nuclear magnetic resonance (NMR) spectroscopy and thus its powerful use in organic and biochemistry.

It is of great interest to find out whether some nuclear spin selection rules exist in the most violent molecular interactions, that is, chemical reactions. Here, not only the energy of interaction, which is on the order of several eV, is much higher than in radiative and collisional interactions, but also the identities of molecules do not remain the same. The quantum numbers related to angular momentum and parity for individual molecules do not have the same meaning for reactants and products. Clearly there are no selection rules for angular momentum and parity for individual molecules except for the conservation of the overall angular momentum and parity. For nuclear spin, however, there still may be some selection rules since all through the process of reaction, permutations of some identical particles are valid operations, the spin statistical requirements are fulfilled, and the nuclear spin interaction energy remains much smaller than the separations of relevant levels.

The existence of such selection rules has been anticipated by Quack in a theoretical paper published in 1977.[9] In this classic paper, Quack discussed ''a simple general method for obtaining selection rules for the ro-vibronic states of reactant and product molecules connected in a reactive collision'' based on the group theory of permutation-inversion operations developed by Hougen,[10] Longuet-Higgins,[11] and Watson[12] as guiding principles. Using many radical and ion–molecule reactions as examples, Quack has demonstrated that ''rather stringent restrictions are found to occur in systems involving three and more identical particles.'' So far no experimental study on this subject seems to have been performed in the gas phase, except for a photodissocation study in formaldehyde by Schramm, Bamford, and Moore.[13] In their work, *ortho*- and *para*-formaldehyde were each selectively photodissociated by tuning a dye laser to either an *ortho*- or *para*-formaldehyde absorption. The H_2 produced was collected and analyzed and it was found that *ortho*-formaldehyde gave pure *ortho*-H_2. However, nonthermal formaldehyde that was enriched in the *para* spin modification was not observed, since the conversion between the two modifications due to collision was too rapid under the experimental conditions used in their measurements. The *para*-H_2-induced polarization observed in NMR spectroscopy[14] is a manifestation of such an effect in the condensed phase.

In this paper, we give experimental evidence that nuclear spin selection rules hold for gas-phase chemical reactions. Preliminary results have been published in an earlier paper.[15] Our results address Quack's theory more directly than those of Schramm *et al.*[13] because (a) we study a chain of ion-neutral reactions in which protons are scrambled rather than the single step photodissociation step in which H_2 is kept as a unit, and (b) we study the spin modification of the polyatomic molecule H_3^+. The experiment was conducted in pure hydrogen plasmas where H_3^+ was produced using either *para*-H_2 or normal H_2 (hereafter abbreviated as p-H_2 and n-H_2) as the discharge gas. H_3^+ is formed by the well-known, efficient ion–molecule reaction

$$H_2+H_2^+ \xrightarrow{k_1} H_3^+ + H, \tag{1}$$

and according to the paper by Quack,[9] only *para*-H_3^+ ($I=1/2$) (p-H_3^+) is expected to form when both reactants are *para* ($I=0$)

$$p\text{-}H_2 + p\text{-}H_2^+ \rightarrow p\text{-}H_3^+ + H. \tag{2}$$

Our experimental results have verified this to be true, although a chain of ensuing reactions between H_3^+ and H_2 complicates the issue as discussed below.

H_3^+ is the simplest stable polyatomic molecular system and has been much studied both theoretically and experimentally.[16–20] It is of great astrophysical interest because it plays the central role in the ion–molecule reaction scheme in the interstellar medium where it has recently been detected.[21,22] The selection rules of nuclear spin symmetry in chemical reactions are especially significant because they are related to the thermalization of nuclear spin modifications of fundamental interstellar molecules such as H_2, H_3^+, NH_3, and H_2CO. For instance, Tennyson, Miller, and Schild report that a difference in the *ortho*-to-*para* ratio of H_3^+ exists between self-thermalized H_3^+ and H_3^+ formed from H_2 produced at the low temperatures of interstellar dust.[23] If H_3^+ thermalizes via proton hopping

$$\tilde{H}_2 + H_3^+ \xrightarrow{k_H} \tilde{H}_2 H^+ + H_2, \tag{3}$$

as has been widely assumed,[24–26] only p-H_3^+ is produced from p-H_2 according to Quack's theory. On the other hand, the hydrogen exchange reaction

$$\tilde{H}_2 + H_3^+ \xrightarrow{k_E} H_2\tilde{H}^+ + H\tilde{H} \tag{4}$$

produces a fraction of o-H_3^+ from p-H_2 and p-H_3^+.

H_3^+ produced from n-H_2 at room temperature in our plasmas exists in a 1:1 ratio of *ortho* ($I=3/2\ A_1'$, spin statistical weight 4) and *para* ($I=1/2\ E'$, spin statistical weight 2) spin modifications.[4] In a totally symmetric vibronic state, the A_1' species combine with the $K=3n$ rotational levels and the E' with the $K=3n\pm1$ levels. Because twice as many $K=3n\pm1$ levels are populated as $K=3n$ at high temperatures, the *ortho*-to-*para* ratio in H_3^+ is 1:1. This nuclear spin distribution is called thermal. If the *ortho*-to-*para* ratio of H_3^+ is not 1:1 at high temperatures, the distribution is nonthermal.

Until now, H_2 and its isotopomers have been the only molecule that can be readily produced and maintained in a nonthermal nuclear spin distribution. Thermal H_2 exists in a

3:1 ratio of *ortho* ($I=1$) and *para* ($I=0$) at high temperatures. When cooled to 20 K or lower in the presence of catalysts such as metal oxides, practically all the molecules occupy the $J=0$ level to form essentially 100% p-H_2. This distribution is thermal at these temperatures. However, when the pure p-H_2 is brought back to room temperature it stays p-H_2 for a long time ($\gtrsim 1$ year) as initially demonstrated by Bonhoeffer and Harteck[27] in 1929. Other instances of nonthermal nuclear spin behavior have been reported in CH_3F,[8,28] D_2O,[29] Na_2 vapor,[30] and Li_2.[31]

For our study of nuclear spin selection rules, we compared the relative intensities of *ortho*- and *para*-H_3^+ transitions obtained in n-H_2 (75% *ortho*, 25% *para*) and p-H_2 plasmas. If the *ortho*-to-*para* H_3^+ intensity ratio is different for the two plasmas, nonthermal steady-state H_3^+ has been produced. n-H_2 would produce thermal H_3^+ (1:1 *ortho*-to-*para* ratio), while p-H_2 would produce nonthermal H_3^+ (*ortho*-to-*para* ratio < 1) if nuclear spin selection rules such as Eq. (2) are obeyed.

We first performed a set of experiments in steady-state positive column and hollow cathode plasmas, which has demonstrated that nuclear spin memory persists even after a series of plasma chemical reactions as anticipated and theoretically formulated by Quack.[9] Solutions of steady-state simultaneous rate equations, in which the *ortho* and *para* spin modifications were treated as separate entities both for H_2 and H_3^+ and their nuclear spin branching ratios calculated according to Quack's theory, qualitatively explained the experimental results. However, steady-state observations have a crucial drawback in that the pure p-H_2 gas led into the plasmas was converted to o-H_2 through a chain of chemical reactions, thus reducing the purity of p-H_2. This greatly reduced the nonthermal distribution and muddled the analysis since the degree of conversion could not be measured *in situ* in plasmas. These steady-state results have been unambiguously corroborated and completed by a second set of experiments using pulsed plasmas in which the pulse width (15 μs–2 ms) is sufficiently short that the conversion of p-H_2 to o-H_2 during the pulse is not overwhelming, and the pulse interval ($\sim$1 s) is sufficiently long that the reaction products are exhaustively pumped out by the time the next pulse is started. This increases the nonthermal distribution of the *ortho*- and *para*-H_3^+ and allows a more clear-cut analysis. Moreover, by using a pulsed discharge current with short rise and fall times (~ 1 μs), a detailed time evolution of the intensities of *ortho*- and *para*-H_3^+ can be studied during and after the pulse. Thus, the analysis of the temporal variations of the $[o\text{-}H_3^+]/[p\text{-}H_3^+]$ ratio is possible.

The rest of the paper is organized as follows: Sec. II describes our apparatus and procedures for both the steady-state and time-dependent experiments in normal and parahydrogen plasmas. Section III presents the observed results and the differences in the H_3^+ *ortho*-to-*para* ratios between n-H_2 and p-H_2 plasmas due to the existence of nuclear spin selection rules in the chemical reactions. These reactions are considered in detail in Sec. IV, paying special attention to the nuclear spin branching ratios. Section V presents the corresponding rate equations and the model we used to interpret our experimental data. Last, the analysis of our results is presented in Sec. VI, and Sec. VII concludes the paper.

TABLE I. H_3^+ *ortho–para* pairs of transitions used in the measurements. Frequencies are in cm^{-1}. See the text for notation.

	Ortho-H_3^+		*Para*-H_3^+	
	Transition	Frequency	Transition	Frequency
(1) $v_2 \leftarrow 0$	$R(1,0)$	2725.898	$R(1,1)^+$	2726.219
(2) $v_2 \leftarrow 0$	$R(4,3)^-$	2894.610	$R(4,4)^-$	2894.488

II. EXPERIMENT

A. Difference frequency spectrometer

A difference frequency laser system has been used as the tunable infrared source to observe *ortho*- and *para*-H_3^+ absorption lines. Details of this spectrometer have been described in previous papers.[32] Briefly, radiation from a single-mode argon ion laser and a tunable ring dye laser are combined in a temperature-controlled $LiNbO_3$ crystal. A few hundred microwatts of infrared is generated from 2.2 to 4.4 μm with a frequency equal to the difference between the frequencies of the argon ion and dye lasers.

B. Parahydrogen preparation

Normal hydrogen was converted into nearly pure (99.8%) parahydrogen by keeping it in contact with nickel silica (Apachi)[33] below 20 K. This paramagnetic catalyst was confined in a copper converter cell inserted in a liquid helium container. Its temperature was monitored by a silicon diode sensor and adjusted by changing the height of the converter over the surface of the liquid helium. The cell was filled with purified hydrogen gas ($<$1 ppm impurity) liquefied inside the converter at $\sim$18 K. The converter cell was then completely submerged in liquid helium and allowed to sit for a few hours or overnight for equilibration. The p-H_2 gas was then obtained by slowly increasing the temperature of the converter and flowed directly into the discharge cells.

C. H_3^+ production and spectroscopy

The H_3^+ ions were generated either in the positive column of a glow discharge[34] or in a hollow cathode[35] discharge as H_2 gas was continuously flowed into the discharge cell and removed by a rotary pump. In order to measure the variation of relative intensities reliably, pairs composed of an o-H_3^+ and a p-H_3^+ line that were within a fraction of a wave number from each other were chosen so that they could both be observed on the same scan. A list of the selected H_3^+ transitions[36] is given in Table I. The notation $R(J,k)^+$ represents the usual perpendicular $J+1 \leftarrow J$, $(k \pm 1, l = \pm 1) \leftarrow k$ transitions except that, since the two excited states of $(k \pm 1, l = \pm 1)$ are badly mixed by the systematic l-resonance interaction,[37,38] Watson's U notation,[38] $+$ or $-$, is used which simply shows the order of energy levels.

D. Steady-state experiments

For steady-state experiments, the positive column discharge was powered by a high-voltage transformer connected to a high-power audio amplifier. The peak-to-peak voltage was a few kilovolts with a current of 200 mA in ~1 torr of hydrogen. For the hollow cathode discharge a peak current of 1.75 A was obtained in ~1.1 torr of hydrogen with a commercial high-voltage ac power supply operating at a few hundred volts. The kinetic temperatures of H_3^+ were approximately 500 and 400 K for the positive column and hollow cathode discharges, respectively.

For both plasmas, a multipass configuration of the radiation was used. In the positive column discharge, H_3^+ signals were observed using the velocity modulation technique[39] with the ac discharge being operated at 6 kHz. The infrared probe beam was initially divided into two beams of approximately equal power by a ZnSe beamsplitter. Each of them traversed the cell four times unidirectionally in opposing directions and were sent to two matched InSb detectors.[32] Signals were then combined 180° out-of-phase in a pair of audio-frequency transformers and sent to a lock-in amplifier. In the hollow cathode, H_3^+ absorption signals were detected using concentration modulation at 10 kHz.[40] One half of the infrared underwent 16 traversals in a standard White cell configuration[41] through the cell and then combined with the other half beam for noise subtraction.

The relative intensities of the pairs of transitions listed in Table I were measured by using alternatively n-H_2 and p-H_2 as the discharge gas every two or three scans (see Fig. 1). Since p-H_2 gas was introduced into the discharge cell directly from the converter by manually adjusting the depth of the converter within the liquid helium bath, the pressure tended to fluctuate a little, causing error in the intensity measurements. This and the fluctuation of infrared power of up to 10% during slow scans caused the main uncertainties in the intensity measurements.

E. Time-dependent experiments

Time-dependent studies were performed in the hollow cathode using basic electronic circuits[42] to produce short and intense current pulses. 15 to 180 μs square pulses with minimal distortion were obtained at 1 Hz for a current and a voltage ranging from 15 to 8 A and 1.4 to 1.2 kV, respectively. Longer 200 μs to 2 ms pulses were best obtained with a current and a voltage ranging from 10 to 1 A and 1.4 to 1.1 kV. Fluctuations in the pulse height could be maintained to within $\pm$5% while the current rise and fall times were on the order of 1 μs and the current was well stabilized after ~5 μs (see Figs. 2 and 3). The discharge was less stable for frequencies outside of the 1–5 Hz range and did not extend sufficiently in the hollow cathode for pulses shorter than 10 μs or longer than 2 ms. The amplitude of the current was largely independent of the gas pressure under 2 torr, but the discharge was less stable below 1 torr. All observations were made at 1.85 torr, where the pulses had the best stability and shape.

The intensities of the H_3^+ lines were monitored using an InSb infrared photovoltaic detector (Graseby Infrared Inc.) after multipassing the infrared beam 16 times in the hollow cathode using a White cell arrangement. Output signals were recorded and averaged directly by a 500 MHz–1 GS/s Tektronix TDS 540 digital oscilloscope triggered by the onset of the current while the laser frequency was fixed at the peak of one of the H_3^+ transitions. Signals were accumulated five to ten times before being transferred to a PC for storage and analysis. Any amplification or signal processing that could affect the linearity or the bandwidth of the detector ($\gtrsim$1 MHz) was avoided. The experimental setup was carefully grounded and shielded to avoid electromagnetic pickup from the intense discharges induced in the hollow cathode. The most sensitive element, i.e., the detector, was confined in a grounded μ-metal box.

One major problem was the background radiation from plasmas to which the detector was also sensitive. In order to minimize this effect, we recorded the background noise at off-resonant positions and subtracted it from the signals using the digital oscilloscope. This procedure, carried out for each measurement, also eliminated other systematic noise and remained effective over the acquisition time. The accuracy of relative intensity measurements was also improved by minimizing the effect of infrared power fluctuations with a faster frequency scan and a quick interchange of discharge gases between successive scans. The hydrogen was flowed into the hollow cathode at the rate of 1.1 L min^{-1} (measured at atmospheric pressure) so that the gas in the hollow cathode was completely renewed in less than 500 ms. Adopting a 1 Hz discharging frequency guaranteed that all reaction products were evacuated and replaced by pure p-H_2 before each new pulse.

III. OBSERVED RESULTS

A. Steady-state experiments

Figures 1(a) and 1(b) show the $R(1,0)/R(1,1)^+$ pair of transitions observed in the positive column and hollow cathode, respectively, illustrating the nonthermal nuclear spin behavior of H_3^+ in the p-H_2 plasmas. The top traces correspond to the scans obtained using n-H_2 as the discharge gas and the bottom to p-H_2. The relative amplitude of the two traces in the figures have been adjusted such that the o-H_3^+ line has the same intensity for the two discharge gases. As mentioned in the Introduction, H_3^+ intensities in n-H_2 correspond to a thermal H_3^+ nuclear spin distribution.

All scans clearly indicate larger p-H_3^+ concentrations in the p-H_2 discharge, showing the existence of selection rules. No appreciable difference in linewidths between o-H_3^+ and p-H_3^+ lines had been detected; therefore, the relative intensities were measured simply from the peak heights.

Table II summarizes the average *ortho*-to-*para* intensity ratios, $\rho = I_{o\text{-}H_3^+}/I_{p\text{-}H_3^+}$, obtained for the various transitions studied. The average *ortho*- to *para*-H_3^+ intensity ratio for $J=1$ is lower by ~34% in the positive column discharge with p-H_2 as the discharge gas compared to n-H_2, while in the hollow cathode, it is by ~20%. This difference is likely due to combined effects of the higher rate of conversion of p-H_2 to o-H_2 in hollow cathode plasmas in which the walls are metallic, and of the slower pumping speed.

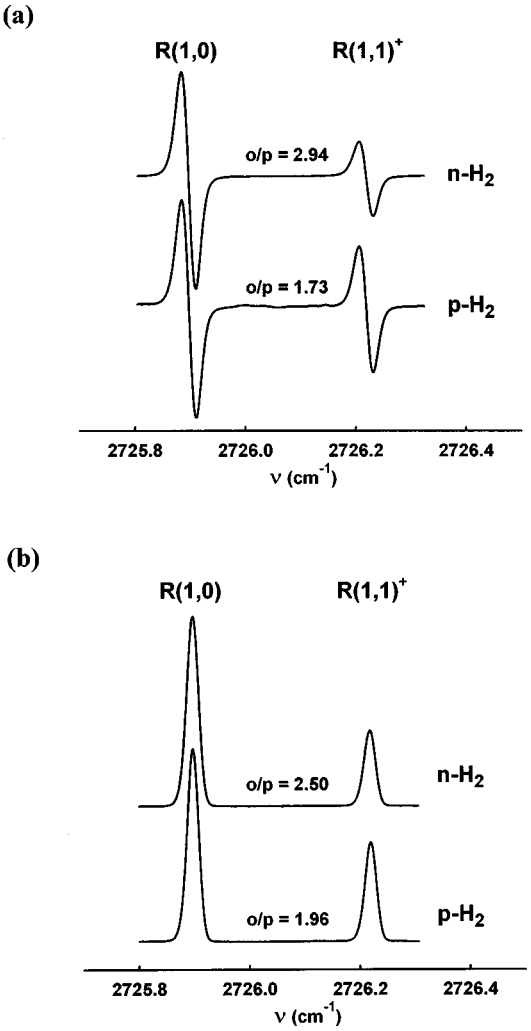

FIG. 1. The observed $R(1,0)$ line of o-H_3^+ and the $R(1,1)^+$ line of p-H_3^+ using n-H_2 (upper trace) and p-H_2 (lower trace) as discharge gases in (a) a positive column and (b) a hollow cathode plasma. The relative amplitude of the traces have been adjusted such that the o-H_3^+ line has the same intensity in both the n-H_2 and the p-H_2 plasmas. The decreased *ortho*- to *para*-H_3^+ intensity ratios for the p-H_2 discharges (lower traces) compared to the n-H_2 discharges (upper traces) demonstrate the existence of selection rules for nuclear spin modifications.

From the observed intensity ratios of o-H_3^+ and p-H_3^+ spectral lines, ρ, the concentration ratios of *ortho*- and *para*-H_3^+ and the fractions of p-H_3^+ for the p-H_2 discharge are determined as

$$\frac{[o\text{-}H_3^+]}{[p\text{-}H_3^+]}=\frac{\rho_{p\text{-}H_2}}{\rho_{n\text{-}H_2}}=R \quad \text{and} \quad \frac{[p\text{-}H_3^+]}{[H_3^+]}=\frac{1}{1+R}, \tag{5}$$

where $\rho_{p\text{-}H_2}$ and $\rho_{n\text{-}H_2}$ are the *ortho*-to-*para* H_3^+ intensity ratios for the p-H_2 and n-H_2 discharges, respectively.

The o-H_3^+ to p-H_3^+ concentration ratios for each pair of transitions are summarized in the last column of Table II. Their deviations from the thermal value of 1 demonstrate the degree of nonthermal nuclear spin distribution of H_3^+ in the p-H_2 plasmas. Their proximity to 1 indicates thermalization subsequent to the reaction of Eq. (1), for otherwise, the fraction of o-H_3^+ to p-H_3^+ ratio would be 0. This fraction is indeed much smaller in the following pulsed experiments, where the effect of p-H_2 to o-H_2 thermalization is much smaller.

TABLE II. Observed average intensity ratios *ortho*-to *para*-H_5^+ lines n-H_2 and p-H_2 discharges and corresponding $[o\text{-}H_3^+]/[p\text{-}H_3^+]$ concentration ratios in steady-state p-H_2 discharges. The numbers following the ± sign refer to the standard deviation. The deviation of the ratio from 1 demonstrates the nuclear spin selection rules.

Transition	n-H_2	p-H_2	$[o\text{-}H_3^+]/[p\text{-}H_3^+]$
	Positive column		
$R(1,0)/R(1,1)^+$	3.09±0.40	2.05±0.45	0.66±0.17
$R(4,3)^-/R(4,4)^-$	0.67±0.11	0.50±0.10	0.75±0.19
	Hollow cathode		
$R(1,0)/R(1,1)+$	2.52±0.34	2.01±0.15	0.80±0.12

B. Pulsed experiments

1. Time dependence of the signals

Typical examples of the time evolution of the o-H_3^+ $R(1,0)$ absorption (lower row) and the p-H_3^+ $R(1,1)^+$ absorption (upper row) are shown in Fig. 2. The pulse current of ~2.8 A and width of 1 ms were used with n-H_2 (left column) and p-H_2 (right column) as discharge gases. A large

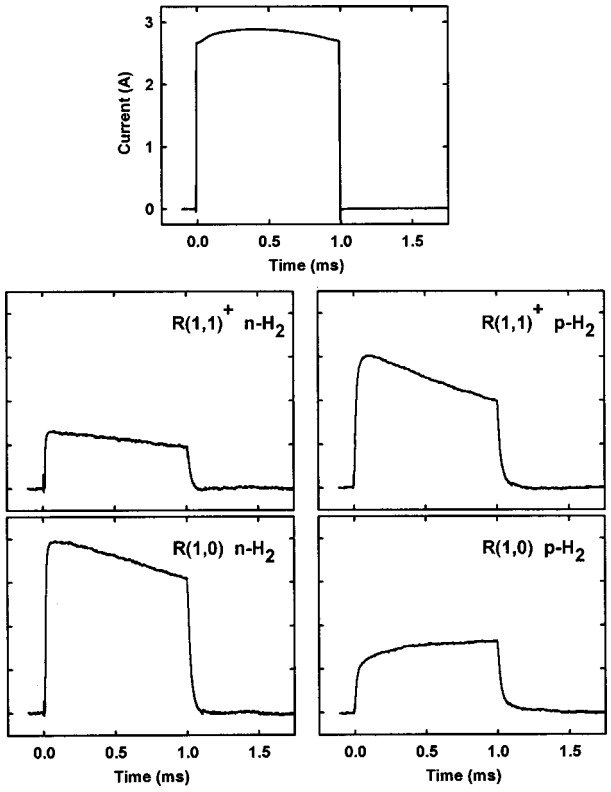

FIG. 2. Observed time variation of the peak intensities of the $R(1,1)^+$ p-H_3^+ infrared absorption (upper traces) and the $R(1,0)$ o-H_3^+ absorption (lower traces) when n-H_2 (left traces) and p-H_2 (right traces) were used as discharge gases. Each trace is the average of ten scans. The absorption intensities are in an arbitrary scale which is common to all four traces. The increase and decrease in intensities of the p-H_3^+ and o-H_3^+ line, respectively, when p-H_2 is used instead of n-H_2 demonstrate the existence of nuclear spin selection rules in ion-neutral reactions.

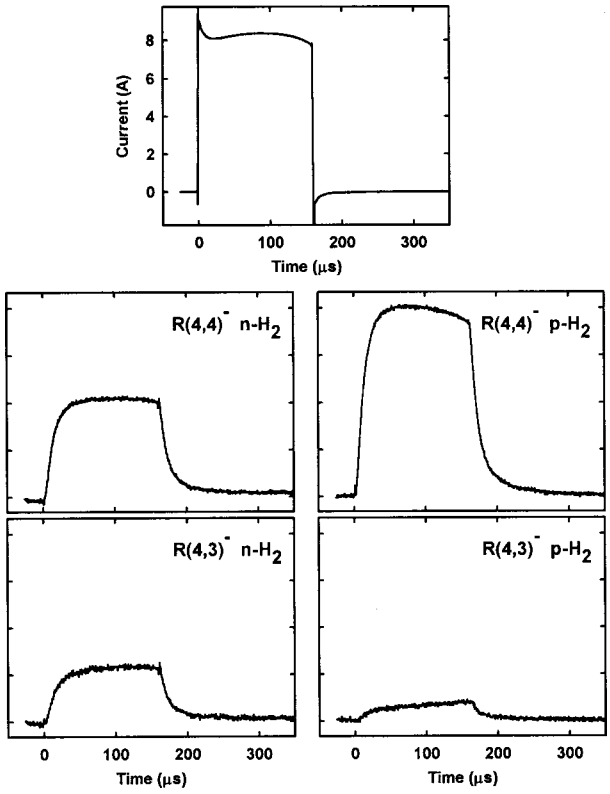

FIG. 3. Same as Fig. 2 except that the $R(4,4)^-$ p-H_3^+ absorption (upper traces) and the $R(4,3)^-$ o-H_3^+ absorption (lower traces) are used.

difference in the relative intensities of the o-H_3^+ and p-H_3^+ absorption was observed depending on whether n-H_2 or p-H_2 was used, clearly demonstrating the existence of selection rules on nuclear spin modifications in plasma chemistry. The intensity of the p-H_3^+ absorption *increases* by a factor of ~ 2, while that of the o-H_3^+ absorption *decreases* by a factor of ~ 3 when p-H_2 is used instead of n-H_2, and the intensity ratio $\rho = I_{o\text{-}H_3^+}/I_{p\text{-}H_3^+}$ is reduced from ~ 3.2 to ~ 0.5. The subtle differences in the time dependence of each signal will be discussed later in this section.

The time dependence of the $J=4$ *ortho/para* H_3^+ pair of transitions $R(4,3)^-/R(4,4)^-$ is shown in Fig. 3. These absorptions are several times weaker than the $J=1$ pair in Fig. 2, and discharge pulses with higher current (8 A) and smaller width (160 μs) were required to observe them with good signal-to-noise ratios. Contrary to the case of the $J=1$ pair, the p-H_3^+ absorption of the $J=4$ pair is stronger than the o-H_3^+ absorption in n-H_2 plasmas. The intensity ratio $\rho = I_{o\text{-}H_3^+}/I_{p\text{-}H_3^+}$, therefore, is very small (1/20–1/10) in p-H_2 plasmas. The observed time dependence of the $J=4$ pair is different from that of the $J=1$ pair because of higher rotational energy. This is further discussed below. As for the $J=1$ pair, an *increase* of the p-H_3^+ signal and a *decrease* of the o-H_3^+ signal are clearly observed when p-H_2 is used instead of n-H_2.

2. o-H_3^+ to p-H_3^+ intensity ratios

The time dependence of the intensity ratios of the o-H_3^+ and p-H_3^+ absorptions are obtained by a simple division of

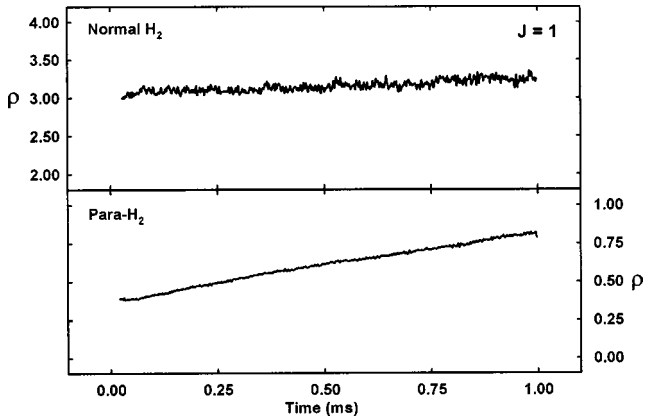

FIG. 4. Observed time dependence of the intensity ratio $\rho(t) = I_{o\text{-}H_3^+}(t)/I_{p\text{-}H_3^+}(t)$ in n-H_2 (upper trace) and p-H_2 plasmas (lower trace) for the $R(1,0)/R(1,1)^+$ pair.

the signals and are shown in Figs. 4 and 5 for the $J=1$ and the $J=4$ pair, respectively. The upper trace of Fig. 4 for the n-H_2 plasma shows that the intensity ratio ρ for the $J=1$ pair is approximately constant and close to its thermal value of 2.94[36] at 300 K throughout the duration of the pulse, as expected. The ratio of 2.94 is simply the ratio of their transition strengths and the nuclear spin states remain thermal. The observed slight increase in the intensity ratio can be ascribed to a plasma heating of the gas which increases the relative population of the $J=1$, $K=0$ H_3^+ slightly with respect to the $J=1$, $K=1$ H_3^+ because of the small energy difference of 22.84 cm^{-1} between them. When p-H_2 is used as the discharge gas the value of ρ is much smaller than that for n-H_2 throughout the period of the pulse (lower trace of Fig. 4) and demonstrates the existence of spin selection rules. The value of ρ increases from 0.38 to 0.83 approximately linearly with time due to the conversion of p-H_2 to o-H_2 during the pulse duration time of 1 ms. If the duration of the plasma is very long, the ratio will converge to the steady-state value of ~ 2.01 (see Table II).

The observed ratio of $\rho = 0.83$ at the end of the pulse indicates that about 19% of p-H_2 is converted to o-H_2 after 1 ms [see Eq. (11) later]. The very rapid conversion from

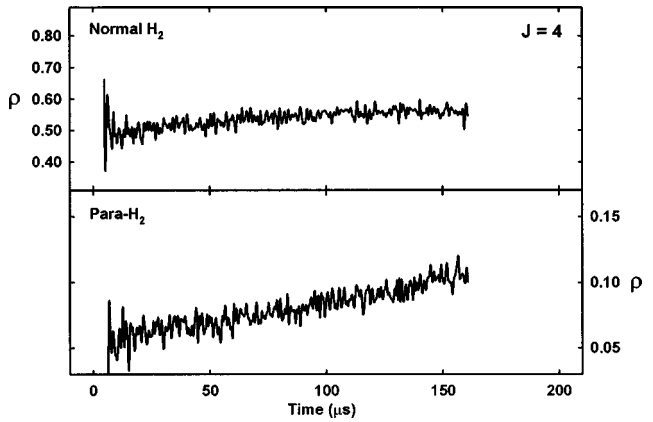

FIG. 5. Observed time dependence of the intensity ratio $\rho(t) = I_{o\text{-}H_3^+}(t)/I_{p\text{-}H_3^+}(t)$ in n-H_2 (upper trace) and p-H_2 plasmas (lower trace) for the $R(4,3)^-/R(4,4)^-$ pair.

p-H_3^+ to o-H_3^+ due to the hydrogen exchange reaction [Eq. (4)] occurs within several microseconds from the onset of the pulse and is not visible in Fig. 4. The initial value of $\rho = 0.38$ represents the state in which p-H_3^+ and o-H_3^+ are equilibrated in a pure p-H_2 plasma.

The time dependence of the intensity ratio $\rho = I_{o\text{-}H_3^+}/I_{p\text{-}H_3^+}$ for the $J=4$ pair is given in Fig. 5. Because of the smaller absorption, the signal-to-noise ratio of ρ is not as good as that for the $J=1$ pair. As in the case of the $J=1$ pair, the value of ρ for the n-H_2 discharge is approximately constant and close to the thermal value of 0.48.[36] The observed slight increase can be explained by plasma heating of the gas; the energy level $(J,K)=(4,3)$ is higher than the (4,4) level by 156.6 cm^{-1}. The p-H_2 discharge (lower trace), on the other hand, gives much lower ρ values due to the spin selection rules. The increase of ρ from 0.053 at the beginning of the pulse to 0.104 after 160 μs corresponds to about 14% conversion of p-H_2 into o-H_2 during the pulse duration [see Eq. (11)]. Compared with the case of the $J=1$ pair, the shorter pulse length is compensated for by the higher current to make the overall effect approximately equal.

3. o-H_3^+ to p-H_3^+ concentration ratios

The time dependence of the o-H_3^+ to p-H_3^+ concentration ratio $R=[o\text{-}H_3^+]/[p\text{-}H_3^+]$ in p-H_2 plasmas can be obtained by dividing the o-H_3^+ to p-H_3^+ intensity ratio in the p-H_2 plasmas, $\rho_{p\text{-}H_2}$, by that in the n-H_2 plasmas, i.e.,

$$R=\rho_{p\text{-}H_2}/\rho_{n\text{-}H_2}.$$

This is because $[o\text{-}H_3^+]=[p\text{-}H_3^+]$ for n-H_2 plasmas in thermal equilibrium. The division eliminates the difference in transition strengths $|\mu|^2$ of the o-H_3^+ and p-H_3^+ absorptions. If we assume the same plasma conditions for the p-H_2 and n-H_2 discharges, the division also eliminates the temperature effect which is weakly observed in the intensity ratios in Figs. 4 and 5. This assumption is probably a good approximation since room temperature is sufficiently high that the thermal properties of o-H_2 and p-H_2 plasmas are not much different.

The time dependence of the o-H_3^+ to p-H_3^+ concentration ratio $R(t)$ thus determined is given in Fig. 6. It is noted that the concentration ratio changed from 0.12 to 0.26 for the $J=1$ pair after 1 ms and from 0.10 to 0.20 for the $J=4$ pair after 160 μs. The ratios for the two pairs are comparable shortly after the onset of the discharge pulse as expected and the difference in the rate of increase 0.14 ms^{-1} and 0.63 ms^{-1} is approximately explained as being due to the difference of the electric currents 2.8 and 8 A, respectively. The ratio should converge to the steady-state value of ~0.80 if the duration of the pulse is very long (see Table II), and to the thermal value of 1 if the gas is not pumped. In view of the large uncertainty for the $J=4$ pair due to the weakness of the signal, we regard these results for the $J=1$ and $J=4$ pairs to be consistent.

We now proceed to examine plasma chemical reactions leading to these experimental results and to understand how H_3^+ ions are thermalized.

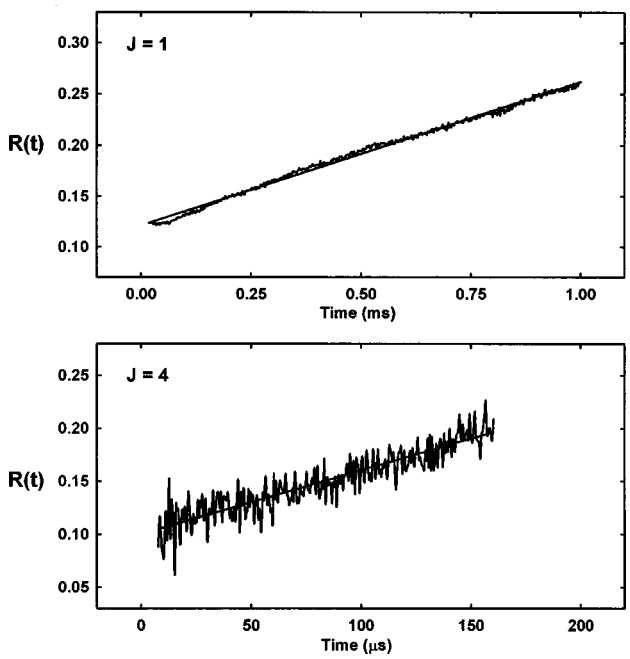

FIG. 6. Observed and calculated (bold line) time dependence of the *ortho*- to *para*-H_3^+ concentration ratio $R(t)=[o\text{-}H_3^+]/[p\text{-}H_3^+]$ in *para*-H_2 plasmas for the $R(1,0)/R(1,1)^+$ pair (upper trace) and the $R(4,3)^-/R(4,4)^-$ pair (lower trace).

IV. PLASMA CHEMICAL REACTIONS INVOLVING H_3^+

The plasma chemistry of H_3^+ begins with the production of H_2^+ by electron impact ionization of H_2. The H_2^+ molecules thus formed react with H_2 to form H_3^+ [Eq. (1)], which then undergo a series of reactions with H_2 where its nuclear spins may be thermalized. The H_3^+ are finally destroyed by dissociative recombination with electrons. We will follow the processes paying special attention to spin modifications. Since our experimental results are not sufficiently detailed or accurate to determine individual nuclear spin branching ratios, we assume Quack's theory to be valid and show that it explains our observations.

A. Electron impact ionization of H_2

H_2^+ is produced by the electron impact ionization of H_2 by energetic electrons

$$H_2+e\xrightarrow{k_i}H_2^++2e. \tag{6}$$

In the positive column, this process is effected by the tail of the Maxwellian energy distribution of electrons with the average energy of 2–3 eV. In the hollow cathode, ''hot'' electrons ejected from the cathode (primary electrons) and from H_2 molecules by electron impact or UV photoionization (secondary electrons) effect the ionization. In calculating the efficiency of ionization we assume the energy distribution of these hot electrons to be Maxwellian. Thus, the electron impact ionization rate constant k_i is calculated from[43]

$$k_i=\frac{1}{n_e}\int \sigma(E)v\, dN, \tag{7}$$

where n_e is the number density of electrons, $\sigma(E)$ is the energy-dependent ionization cross section,[44] v is the average velocity of electrons, and dN is the Maxwellian number density of electrons at the velocity v. Using the values given by Rapp and Englander-Golden[45] and Kieffer,[44] the ionization rate constant k_i is calculated to be $2.5\times10^{-11}\,\mathrm{cm^3\,s^{-1}}$ in the positive column discharge, assuming the average electron energy of 2.5 eV. The ionization rate constants in the hollow cathode have been discussed earlier.[35] Assuming average energies of 40 and 4 eV, respectively, for the primary and the secondary electrons in the hollow cathode, we obtain rate constants of $k_{i1}=2.8\times10^{-8}\,\mathrm{cm^3\,s^{-1}}$ and $k_{i2}=3.1\times10^{-10}\,\mathrm{cm^3\,s^{-1}}$, respectively. Since electron impact ionization is very fast compared to the reorientation of nuclear spins, H_2^+ ions retain the nuclear spin modification of the reacting H_2 molecule; that is, only p-H_2^+ are produced from p-H_2.

B. H_3^+ production

H_3^+, the most abundant molecular ion in hydrogen discharges,[46] is produced by the ion–molecule reaction of Eq. (1). It is exothermic by 1.7 eV and proceeds with the large Langevin rate with the rate constant of $k_1=2.0\times10^{-9}\,\mathrm{cm^3\,s^{-1}}$.[47] The reaction can be regarded either as a proton hop reaction,

$$\tilde{H}_2+H_2^+\rightarrow\tilde{H}_2H^++H, \tag{1a}$$

or as a hydrogen abstraction reaction,

$$\tilde{H}_2+H_2^+\rightarrow\tilde{H}H_2^++\tilde{H}. \tag{1b}$$

Experimental studies using isotopes have shown that their branching ratio is ~1:1.[48–50] Quack has shown that if p-H_2 and p-H_2^+ are used, only p-H_3^+ is produced. By using the statistical method similar to that given in Sec. 6 of Quack's paper,[9] we obtain branching ratios for other reactants as

$$p\text{-}H_2+p\text{-}H_2^+ \longrightarrow p\text{-}H_3^++H$$

$$p\text{-}H_2+o\text{-}H_2^+ \xrightarrow{1/3} o\text{-}H_3^++H$$

$$o\text{-}H_2+p\text{-}H_2^+ \xrightarrow{2/3} p\text{-}H_3^++H$$

and

$$o\text{-}H_2+o\text{-}H_2^+ \xrightarrow{2/3} o\text{-}H_3^++H$$

$$\xrightarrow{1/3} p\text{-}H_3^++H.$$

Branching ratios for different nuclear spin modifications are the same for (1a) and (1b). These branching ratios are summarized in Table IIIa. More details of the theoretical basis of the calculations will be given in a separate paper.

TABLE III. Branching ratios of spin modifications based on Quack's theory

(a)

$H_2+H_2^+\rightarrow H_3^++H$

Spin species[a]	Weight	*o*[b]	*p*
oo	9	6	3
op	3	1	2
po	3	1	2
pp	1	0	1

(b)

$H_3^++H_2\rightarrow H_3^++H_2$

spin species[c]	Weight	*oo*[d]	*op*	*po*	*pp*
oo	12	37/5	1	14/5	4/5
op	4	1	1	2	0
po	12	14/5	2	28/5	8/5
pp	4	4/5	0	8/5	8/5

[a]*oo*, etc., denote reactions of o-H_2 and o-H_2^+, etc.
[b]*o*,*p* denote the product o-H_3^+, p-H_3^+.
[c]*oo*, etc., denote reactions of o-H_3^+ and o-H_2, etc. in that order.
[d]*oo*, etc., denote the products o-H_3^+ and o-H_2, etc., in that order.

C. Reactions of H_3^+ and H_2

The H_3^+ ions thus produced undergo many ion-neutral reactions with H_2 through the proton hop reaction Eq. (3), and the hydrogen exchange reaction Eq. (4). The total rate of the reactions has been reported by many authors using isotopes,[47] but we adopt here the value of $k_2=k_E+k_H=1.3\times10^{-9}\,\mathrm{cm^3\,s^{-1}}$ measured by Adams and Smith.[51] The branching ratios of nuclear spin modifications for the total process based on Quack's theory are given in Table IIIb. In this calculation a complete scrambling of the five protons in the transition state H_5^+ is assumed and the subtleties of the chemical reactions on the potential surfaces are ignored. While Quack focuses his argument on symmetries of rovibronic states, we concentrate on symmetries of nuclear spin states. Since we are interested in the measurement of o-H_3^+ and p-H_3^+, we ignore the difference in o-H_2 and p-H_2 in the product and thus sum the columns $oo+op$ and $po+pp$ in Table IIIb. In order to take into account the subtlety of chemistry, we separate the total branching ratios into three cases—no reaction, the proton hop reaction, and the hydrogen exchange reaction with statistical weights of 1:3:6, respectively. Since calculating the o-H_3^+ to p-H_3^+ branching ratios for the first two processes is trivial, we thus obtain the branching ratios summarized in Table IV. The proton hop reactions with p-H_2 always give p-H_3^+. The hydrogen exchange reaction, however, gives a fraction of o-H_3^+ even if p-H_2 and p-H_3^+ react. *Since this is the only ion-neutral reaction that introduces* o-H_3^+ *in* p-H_2 *plasmas, the ratios of the rate constant for the proton hop reaction,* k_H, *and that for the hydrogen exchange reaction,* k_E, *is crucial in the resultant* o-H_3^+/p-H_3^+ *ratio*. We have determined this ratio to be $k_H/k_E\sim2.4$ from the time-dependent measurement (see

TABLE IV. Nuclear spin branching ratios for the $H_3^+ + H_2 \rightarrow H_3^+ + H_2$ reaction.

o-$H_3^+ + o$-H_2				
proton hop	$\rightarrow$	$\frac{2}{3}$	o-$H_3^+ + \frac{1}{3}$	p-H_3^+
hydrogen exchange	$\rightarrow$	$\frac{2}{3}$	o-$H_3^+ + \frac{1}{3}$	p-H_3^+
no reaction	$\rightarrow$		o-H_3^+	
o-$H_3^+ + p$-H_2				
proton hop	$\rightarrow$			p-H_3^+
hydrogen exchange	$\rightarrow$	$\frac{2}{3}$	o-$H_3^+ + \frac{1}{3}$	p-H_3^+
no reaction	$\rightarrow$		o-H_3^+	
p-$H_3^+ + o$-H_2				
proton hop	$\rightarrow$	$\frac{2}{3}$	o-$H_3^+ + \frac{1}{3}$	p-H_3^+
hydrogen exchange	$\rightarrow$	$\frac{1}{3}$	o-$H_3^+ + \frac{2}{3}$	p-H_3^+
no reaction	$\rightarrow$			o-H_3^+
p-$H_3^+ +$ p-H_2				
proton hop	$\rightarrow$			p-H_3^+
hydrogen exchange	$\rightarrow$	$\frac{1}{3}$	o-$H_3^+ + \frac{2}{3}$	p-H_3^+
no reaction	$\rightarrow$			p-H_3^+

Sec. VI). We thus use $k_H = 9.2\times10^{-10}\,cm^3\,s^{-1}$ and $k_E = 3.8\times10^{-10}\,cm^3\,s^{-1}$ in the analysis of our steady-state experiment.

D. Dissociative recombination

H_3^+ ions are destroyed by dissociative recombination

$$H_3^+ + e \xrightarrow{k_r} H_2 + H$$
$$\rightarrow H + H + H, \tag{9}$$

either in the bulk plasma or on the wall. The past several years have seen a controversy over the rate constant for this reaction, whose values have varied from $\sim10^{-7}\,cm^3\,s^{-1}$ (Ref. 52) to $10^{-11}\,cm^3\,s^{-1}$ (Ref. 53) and back to $10^{-7}\,cm^3\,s^{-1}$ (Refs. 54–57) at 300 K. Here, we use Amano's value[55] of $k_r = 1.8\times10^{-7}\,cm^3\,s^{-1}$ which was obtained in a hollow cathode discharge similar to ours. With an assumed ultimate electron density of $6.0\times10^{11}\,cm^{-3}$ in the hollow cathode,[35] this gives the estimated lifetime of H_3^+ to be 9 μs. In the positive column plasma where the electron density is an order of magnitude smaller ($3\times10^{10}\,cm^3$), the main destruction mechanism is the dissociative recombination on the wall which is governed by the ambipolar diffusion rate estimated to be $\gamma \sim 4.8\times10^5\,s^{-1}$ corresponding to the lifetime of 2 μs. Using the total rate constant for the $H_3^+ + H_2$ reaction of $1.3\times10^{-9}\,cm^3\,s^{-1}$ and the H_2 number densities of $1.2\times10^{16}\,cm^{-3}$ and $3.6\times10^{16}\,cm^{-3}$ for the positive column and hollow cathode, respectively, we find that H_3^+ ions undergo reactions over 100 times during their lifetimes.

E. Conversion of p-H_2 to o-H_2

So far we have focused our argument on the concentration of o-H_3^+ and p-H_3^+ but reactions in Eqs. (3) and (4) convert o-H_2 and p-H_2 in an intricate manner. The reactions in Eqs. (1) and (9) produce atomic hydrogen that will recombine on the wall to produce o-H_2 and p-H_2 in the statistical 3:1 ratio. Moreover, the electron impact dissociation reaction

TABLE V. Chemical reactions included in the model calculations.

Equation #			
(1)	$H_2 + H_2^+$	$\xrightarrow{k_1}$	$H_3^+ + H$
(3)	$H_3^+ + \tilde{H}_2$	$\xrightarrow{k_H}$	$\tilde{H}_2H^+ + H_2$
			$(k_2 = k_H + k_E)$
(4)	$H_3^+ + \tilde{H}_2$	$\xrightarrow{k_E}$	$H_2\tilde{H}^+ + H\tilde{H}$
(6)	$H_2 + e$	$\xrightarrow{k_i}$	$H_2^+ + 2e$
(9)	$H_3^+ + e$	$\xrightarrow{k_r}$	H+H+H or H_2+H

$$H_2 + e \rightarrow H + H + e, \tag{10}$$

which is equally efficient as the ionization reaction Eq. (6) will produce copious amounts of H atoms which also recombine to molecular H_2 on the wall. All these reactions thermalize pure p-H_2 into n-H_2.

Since a quantitative treatment of these reactions was difficult, we measured the o-H_2 to p-H_2 ratio of the exhaust gas by the thermometric method.[58] We thus used the p-H_2 fraction of 73% and 67%, respectively, obtained by the thermometric method for the positive column and hollow cathode (see Table VII) for the analysis of the steady-state plasmas. We have also attempted to observe the o-H_2 to p-H_2 ratio *in situ* in plasmas using the $5g$-$4f$ H_2 Rydberg spectrum.[59] The difficulty here was that pairs of Rydberg spectral lines which are accidentally close to each other have different vibrational states and thus their intensity ratios are extremely sensitive to plasma conditions. For pulsed experiments, the p-H_2 concentration of course is 100% at the onset of discharges [see Eq. (11)], and the analysis is more clear-cut.

V. RATE EQUATIONS

The plasma chemical reactions are listed in Table V. The rate equations for these reactions incorporating the nuclear

TABLE VI. Rate equations used in the analysis.

$(d[p\text{-}H_2^+])/dt$	=	$\{k_{i1}[e_1] + k_{i2}[e_2]\}[p\text{-}H_2] - k_1[H_2][p\text{-}H_2^+]$
$(d[o\text{-}H_2^+])/dt$	=	$\{k_{i1}[e_1] + k_{i2}[e_2]\}[o\text{-}H_2] - k_1[H_2][o\text{-}H_2^+]$
$(d[p\text{-}H_3^+])/dt$	=	$k_1(\frac{2}{3}[o\text{-}H_2] + [p\text{-}H_2])[p\text{-}H_2^+]$ $+ k_1(\frac{1}{3}[o\text{-}H_2] + \frac{2}{3}[p\text{-}H_2])[o\text{-}H_2^+]$ $+ \{k_H(-\frac{2}{3}[o\text{-}H_2]) + k_E(-\frac{1}{3}[o\text{-}H_2] - \frac{1}{3}[p\text{-}H_2])$ $- (k_r[e] + \gamma)\}[p\text{-}H_3^+]$ $+ \{k_H(\frac{1}{3}[o\text{-}H_2] + [p\text{-}H_2]) + k_E(\frac{1}{3}[o\text{-}H_2] + \frac{1}{3}[p\text{-}H_2])\}$ $\times [o\text{-}H_3^+]$
$(d[o\text{-}H_3^+])/dt$	=	$k_1(\frac{1}{3}[o\text{-}H_2])[p\text{-}H_2^+]$ $+ k_1(\frac{2}{3}[o\text{-}H_2] + \frac{1}{3}[p\text{-}H_2])[o\text{-}H_2^+]$ $+ \{k_H(\frac{2}{3}[o\text{-}H_2]) + k_E(\frac{1}{3}[o\text{-}H_2] + \frac{1}{3}[p\text{-}H_2])\}[p\text{-}H_3^+]$ $+ \{k_H(-\frac{1}{3}[o\text{-}H_2] - [p\text{-}H_2]) + k_E(-\frac{1}{3}[o\text{-}H_2]$ $- \frac{1}{3}[p\text{-}H_2]) - (k_r[e] + \gamma)\}[o\text{-}H_3^+]$

TABLE VII. Rate constants, measured concentrations of H_2 used in our model and calculated charge concentrations in the positive column and hollow cathode discharges. For time-dependent experiments, number densities shortly after the onset of the pulse are given.

Positive column					Hollow cathode				
Rate constants									
k_i	=	2.5×10^{-11}	$cm^3\,s^{-1}$		k_{i1}	=	2.8×10^{-8}	$cm^3\,s^{-1}$	
					k_{i2}	=	3.1×10^{-10}	$cm^3\,s^{-1}$	
γ	=	4.8×10^{5}	s^{-1}		k_r	=	1.8×10^{-7}	cm^3	
			k_1	=	2.0×10^{-9}		$cm^3\,s^{-1}$		
			k_2	=	1.3×10^{-9}		$cm^3\,s^{-1}$		
Steady-state experiments									
$[H_2]$	=	1.2×10^{16}	cm^{-3}		$[H_2]$	=	3.6×10^{16}	cm^{-3}	
$[p\text{-}H_2]$	=	2.4×10^{16}	cm^{-3}	(73 %)	$[p\text{-}H_2]$	=	2.4×10^{16}	cm^{-3}	(67 %)
$[H_2^+]$	=	3.7×10^{8}	cm^{-3}		$[H_2^+]$	=	8.7×10^{8}	cm^{-3}	
$[p\text{-}H_2^+]$	=	2.7×10^{8}	cm^{-3}		$[p\text{-}H_2^+]$	=	5.8×10^{8}	cm^{-3}	
$[H_3^+]$	=	3.0×10^{10}	cm^{-3}		$[H_3^+]$	=	5.9×10^{11}	cm^{-3}	
$[p\text{-}H_3^+]$	=	2.2×10^{10}	cm^{-3}	(73 %)	$[p\text{-}H_3^+]$	=	4.2×10^{11}	cm^{-3}	(71 %)
$[e]$	=	3×10^{10}	cm^{-3}		$[e]$	=	5.9×10^{11}	cm^{-3}	
					$[e_1]$	=	3.0×10^{7}	cm^{-3}	
					$[e_2]$	=	3.0×10^{9}	cm^{-3}	
Time-dependent experiments									
					$[H_2]$	=	6.0×10^{16}	cm^{-3}	
					$[p\text{-}H_2]$	=	6.0×10^{16}	cm^{-3}	(100 %)
					$[H_2^+]$	=	1.5×10^{9}	cm^{-3}	
					$[H_3^+]$	=	1.0×10^{12}	cm^{-3}	
					$[e]$	=	1.0×10^{12}	cm^{-3}	
					$[e_1]$	=	3.0×10^{7}	cm^{-3}	
					$[e_2]$	=	3.0×10^{9}	cm^{-3}	
					α	=	2.4		
					τ	=	3.5	ms	

spin branching ratios (Table IV) to calculate the concentration of ionic species in the discharge are summarized in Table VI.

The rate constants k_i, k_1, k_H, k_E, and k_r are for the ionization, the ion neutral reaction [Eq. (1)], the proton hop reaction [Eq. (3)], the hydrogen exchange reaction [Eq. (4)] and the electron recombination [Eq. (9)], respectively (Table V). γ gives the rate of destruction of H_3^+ by the recombination on the wall after ambipolar diffusion. The numerical values of these constants together with the measured H_2 concentration $[H_2]=[p\text{-}H_2]+[o\text{-}H_2]$, the p-H_2 concentration $[p\text{-}H_2]$, and the estimated electron concentration $[e]$ are listed in Table VII. Note that $[e_1]$ and $[e_2]$ are estimated concentrations of the primary and secondary electrons, respectively, and $[e]$ is that of low temperature ''ultimate'' electrons. These slow electrons have lost their energies through many inelastic collisions and have energies that are typically much less than 1 eV.[35] The concentrations of the high energy primary and secondary electrons are less than that of ultimate electrons, by approximately 2 and 4 orders of magnitude, respectively.[35]

VI. ANALYSIS

A. Steady-state experiments

We have solved the rate equations in Table VI for steady-state conditions, $(d[\ ]/dt)_{t\to\infty}=0$, using the numerical values in Table VII. Plasma neutrality is assumed by equating the concentrations of electrons with those of H_3^+ and H_2^+ ions in each discharge. The total H_3^+ concentrations in the two plasmas, as well as the *para* concentrations of H_3^+ and H_2^+, are shown in Table VII.

While the nonthermal *ortho*-to-*para* H_3^+ ratio has been demonstrated, the calculated p-H_3^+ concentrations of 73% and 71% from Eq. (5) in the positive column and the hollow cathode, respectively (Table VII), are considerably higher than the average observed values 60% and 56% calculated from Eq. (5) using the $[o\text{-}H_3^+]/[p\text{-}H_3^+]$ ratio R listed in Table II.

There are several factors that contribute to the error in the calculated values of $[p\text{-}H_3^+]/[H_3^+]$. One is the large uncertainty ~10% in the p-H_2 concentration measured by thermal conductivity that translates to the uncertainty of ~7% in the $[p\text{-}H_3^+]/[H_3^+]$ observed value. One other uncertainty that affects the rate of thermalization is related to the spatial macroscopic inhomogeneity of the plasma, which is ignored in this work. Steady-state equations refer to a local microscopic equilibrium for chemical reactions that is extremely fast compared to our measurements. The pumping of the gas and the geometry of the cells can cause spatial inhomogeneity of the plasma, affect the length of time hydrogen remains in the plasma, and thus influence its degree of thermalization. For instance, with its larger volume and the simple construction of the gas inlet and outlet system, gas in the hollow cathode takes longer to be pumped out than in the positive column. During that time, H_2 and H_3^+ can go through more chemical reactions and thermalize more. Thus, obtaining different

ortho-to-*para* H_3^+ ratios in the positive column discharge from those in the hollow cathode discharge is not surprising. Also, the physical and chemical conditions in the two plasmas, one surrounded by a glass wall and the other by a metal wall, are very different. The thermal conductivity measurements have shown that more p-H_2 is converted to o-H_2 in the hollow cathode discharge than in the positive column. Very likely, this is partly due to the more efficient atom recombination on cold, metallic surfaces. Finally, the efficient electron impact dissociation of H_2 and the stability of H atoms in our discharges may make the steady-state concentrations of H atoms much higher than that of H_3^+. These H atoms recombine on the wall and produce the thermal 3:1 spin distribution of H_2.

Taking into account such dynamics in our model would be very difficult. These complications do not occur in the pulsed experiments discussed below in which the thermalization is directly observed.

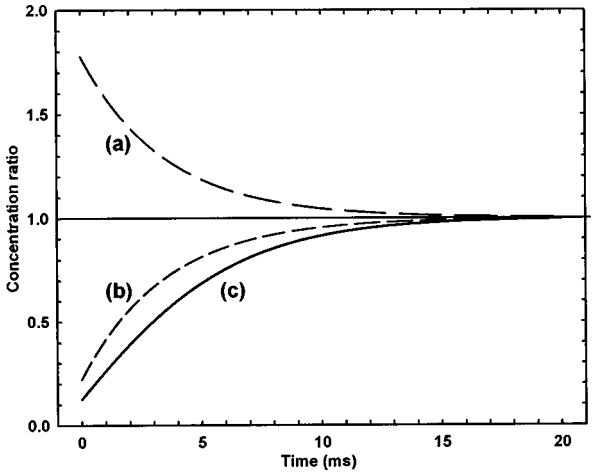

FIG. 7. Simulated time dependence of the concentration ratio (a) 2 $[p\text{-}H_3^+]/[H_3^+]$, (b) 2 $[o\text{-}H_3^+]/[H_3^+]$, and (c) $R(t)=[o\text{-}H_3^+]/[p\text{-}H_3^+]$ in the hollow cathode plasma for the $R(1,0)/R(1,1)^+$ pair.

B. Pulsed experiments

For the analysis of the pulsed experiments, we use the simultaneous rate equations in Table VI, taking into account the time dependence of the number densities of reactants.

The ionization of H_2, reaction (6), in a hollow cathode plasma is affected by the primary electrons e_1 (electrons ejected from cathode with average energy of ~40 eV) and the secondary electrons e_2 (electrons ejected from molecules upon primary ionization with average energy of ~4 eV), whose concentrations were assumed to be proportional to that of ultimate electrons (low temperature electrons which are most abundant[60]), $[e]$, with proportionality factors of $[e_1]/[e]=5\times10^{-5}$ and $[e_2]/[e]=5\times10^{-3}$, respectively. Values of $[e]$ and the ionization rate constants by the primary and the secondary electrons, k_{i1} and k_{i2}, used in this calculation are listed in Table VII. These are rough estimates based on our previous study of hollow cathode plasma chemistry,[35] but the $[o\text{-}H_3^+]/[p\text{-}H_3^+]$ concentration ratio does not depend critically on these estimates. The electron concentration follows the onset of the plasma pulse with a short time delay (few microseconds) and is assumed to reach the steady-state instantaneously. As with the steady-state analysis, literature values are assumed for the rate constants k_1[47] and $k_2=k_H+k_E$,[51] and Amano's value of the recombination rate constant k_r[55] is used as shown in Table VII. Again, the $[o\text{-}H_3^+]/[p\text{-}H_3^+]$ concentration ratio is not very sensitive to these rate constants. *The ratio is critically dependent only on the ratio of the rate constants for the proton hop reaction* k_H *and for the hydrogen exchange reaction* k_E. This is understandable because the latter is the only reaction that converts p-H_3^+ into o-H_3^+ upon reaction with p-H_2. The ratio $\alpha=k_H/k_E$ is determined such that the observed initial values of $R=[o\text{-}H_3^+]/[p\text{-}H_3^+]\sim0.12$ and 0.10 for the $J=1$ and the $J=4$ pairs in the p-H_2 discharge, respectively, (Fig. 6) agree with the calculated values.

The above analysis has a serious omission in that reactions involving hydrogen atoms are not taken into account. The cross section of the electron impact dissociation of H_2 has the same order of magnitude as that of the H_2 ionization. H atoms thus produced together with H atoms from reactions (1) and (9) in Table V will react with other species in plasmas and also recombine on the metal wall of the hollow cathode. Such reactions convert p-H_2 to o-H_2 and cause the time dependence of $[o\text{-}H_3^+]/[p\text{-}H_3^+]$ during the plasma pulse shown in Fig. 6. Since we do not have means to monitor the H atom concentration nor accurate theoretical estimates of reactions involving H atoms, we assume a simple statistical exponential decay of pure p-H_2 to n-H_2 by

$$[p\text{-}H_2]=(1-\tfrac{3}{4}(1-e^{-t/\tau}))[p\text{-}H_2]_0, \tag{11}$$

and determine the time constant τ such that the calculated time dependence of $[o\text{-}H_3^+]/[p\text{-}H_3^+]$ agree with the observed values of Fig. 6.

The time-dependent simultaneous equations in Table V are solved with the constraints of charge neutrality,

$$[e]+[e_1]+[e_2]=[p-H_3^+]+[o\text{-}H_3^+]+[p\text{-}H_2^+]+[o\text{-}H_2^+], \tag{12}$$

and the initial condition

$$[p\text{-}H_2]_0=[H_2] \text{ and } [H_2^+]_0=[H_3^+]_0=[e]_0=0. \tag{13}$$

We then obtain the value of the branching ratio $\alpha=k_H/k_E=2.4$ and the p-H_2 lifetime $\tau=3.5$ ms for the $J=1$ pair, and $\alpha=3.0$ and $\tau=0.8$ ms for the $J=4$ pair. As discussed earlier, the difference in τ for the two cases is due to the difference in discharge current. We regard the difference in the values of α to be within the uncertainties of our experiment. As discussed earlier, measurements for the $J=4$ pair have higher uncertainties and we adopt $\alpha=2.4$ to be the ratio k_H/k_E.

Gerlich has measured the ratio of $\alpha=k_H/k_E$ mass spectroscopically using the $D_3^++H_2$ reaction[61] and reported that α depends critically on the collision energy of the reactants. If we use the results shown in Fig. 10 of Gerlich's paper,[61] we find that our branching ratio $\alpha=2.4$ corresponds to the collision energy of $E_T=\frac{3}{2}k_BT=57$ meV, that is $T\sim440$ K which is in agreement with the estimated temperature of ~400 K in our pulsed hollow cathode plasma.

Using the results of the above model calculation, we can estimate the time dependence of the p-H_3^+ and o-H_3^+ concentrations in our hollow cathode cell. In Fig. 7 curves (a) and (b) give ratios of $[p\text{-}H_3^+]$ and $[o\text{-}H_3^+]$ to their thermal values $[p\text{-}H_3^+]_\infty=[o\text{-}H_3^+]_\infty=[H_3^+]/2$, and (c) gives the ratio of $[o\text{-}H_3^+]/[p\text{-}H_3^+]$. We note that the H_3^+ spin modifications are completely thermalized in ~20 ms. In our steady-state experiment, pumping of the gas maintains the ratio at 0.80 corresponding to $t\sim 6.5$ ms.

While the temporal variation of the concentration ratio $[o\text{-}H_3^+]/[p\text{-}H_3^+]$ during the current pulse has been explained semiquantitatively in the above argument, the decay of the absorption signal after the pulse could not be quantitatively accounted for from the reactions listed in Table VI alone. For this analysis we used the observed time variation of H_3^+ signals in n-H_2 discharges in which spin modifications of both H_2 and H_3^+ remain in their thermal distributions and the complication due to conversion between p-H_3^+ and o-H_3^+ does not exist.

As discussed by Amano,[55] if pure H_2 is used in the discharge, the decay of the H_3^+ signal is due only to electron recombination, for which the rate equation is

$$\frac{d[H_3^+]}{dt}=-k_r[H_3^+][e]=-k_r[H_3^+]^2, \tag{14}$$

and its solution is

$$\frac{1}{[H_3^+]}-\frac{1}{[H_3^+]_0}=k_r t. \tag{15}$$

However, we found that the observed time dependence does not fit this relation well. We also had to assume a large value of $[H_3^+]_0$ if we used this relation and Amano's value of the recombination rate constant $k_r=1.8\times10^{-7}\,\mathrm{cm^3\,s^{-1}}$. Both of these problems are reduced considerably if we take into account the presence of a small amount of impurity in our plasmas. This is possible because, unlike Amano's hollow cathode, which is cooled by liquid nitrogen, ours operate at room temperature and small amounts of H_2O and NH_3 produced from O_2 and N_2 impurity cannot be efficiently eliminated. A similar complication due to water impurity was reported by Fehér, Rohrbacher, and Maier[62] in their H_3^+ recombination measurement. The rate equations are

$$\frac{d[H_3^+]}{dt}=-k_r[H_3^+][e]-k_X[H_3^+][X], \tag{16}$$

$$\frac{d[HX^+]}{dt}=-k_r[HX^+]+k_X[H_3^+][X], \tag{17}$$

where X summarily represents the impurities H_2O,NH_3, etc. which react with H_3^+ with the large Langevin rate constant of $k_X\sim5\times10^{-9}\,\mathrm{cm^3\,s^{-1}}$.[47] Solving the simultaneous equations with the neutrality condition

$$[e]=[H_3^+]+[HX^+], \tag{18}$$

we obtain the time dependence of the H_3^+ concentration as

$$[H_3^+]=\frac{[H_3^+]_0}{1+k_r t[H_3^+]_0}e^{-k_X[X]t}, \tag{19}$$

and this fits better with the observed decay. The best fit to the observed decay is obtained with

$$[H_3^+]_0=3.5\times10^{11}\,\mathrm{cm^3}\ \text{and}\ k_X[X]=3\times10^4\mathrm{s^{-1}};$$
$$\text{that is}\ [X]=6\times10^{12}\,\mathrm{cm^{-3}}. \tag{20}$$

This complication due to the proton hop reaction from H_3^+ to impurities is not discriminative of spin modifications and is not considered in the calculation of the o-H_3^+/p-H_3^+ ratio in the analysis of the pulsed experiments.

VII. CONCLUSION

The relative intensities of o-H_3^+ and p-H_3^+ absorption lines have been measured in steady-state plasmas in positive column and hollow cathode discharges and in pulsed hollow cathode plasmas using pure p-H_2 and n-H_2 as discharge gases. The measurements yielded the steady-state and time-dependent *ortho*-to-*para* H_3^+ concentration ratios $R=[o\text{-}H_3^+]/[p\text{-}H_3^+]$ in the pure p-H_2 discharge which are clearly nonthermal and give clear evidence for the existence of nuclear spin selection rules in hydrogen plasmas.

The value and the time dependence of the *ortho*-to *para*-H_3^+ concentration ratio, $R(t)$, have been analyzed using a simple plasma chemical model in which the conversion from p-H_3^+ to o-H_3^+ due to the scrambling of protons has been taken into account by using the nuclear spin modification branching ratio based on the theory of Quack.[9] The observed values of $R(t)$ depend critically on the ratio of rate constants for the proton hop reaction k_H and for the hydrogen exchange reaction k_E. This ratio $\alpha=k_H/k_E$ has been determined to be ~2.4.

ACKNOWLEDGMENTS

This work has been supported by NSF Grant No. PHY-9722691, NASA Grant No. NAG5-4234, and NATO collaborative research Grant No. CRG 951268 between the Université des Sciences et Technologies de Lille and the University of Chicago.

[1] C. N. Yang, Science **127**, 565 (1958).
[2] G. Herzberg, *Molecular Spectra and Molecular Structure* (Van Nostrand New York, 1966), Vols. I–III.
[3] T. Oka, Adv. At. Mol. Phys. **9**, 127 (1973).
[4] L. D. Landau and E. M. Litshitz, *Quantum Mechanics, Non-relativistic Theory* (Pergamon, New York, 1965). *Ortho*, *meta*, and *para* are named in the order of the abundances of these species at room temperature.
[5] R. F. Curl, Jr., J. V. V. Kasper, and K. S. Pitzer, J. Chem. Phys. **46**, 3220 (1967).
[6] I. Ozier, Phys. Rev. Lett. **27**, 1329 (1971).
[7] J. Bordé, Ch. J. Bordé, Ch. Salomon, A. Van Lerberghe, M. Ouhayoun, and C. D. Cantrell, Phys. Rev. Lett. **45**, 14 (1980).
[8] B. Nagels, N. Calas, D. A. Roozemond, L. J. F. Hermans, and P. L. Chapovsky, Phys. Rev. Lett. **77**, 4732 (1996).
[9] M. Quack, Mol. Phys. **34**, 477 (1977).
[10] J. T. Hougen, J. Chem. Phys. **37**, 1433 (1962).
[11] H. C. Longuet-Higgins, Mol. Phys. **6**, 445 (1963).
[12] J. K. G. Watson, Can. J. Phys. **43**, 1996 (1965).
[13] B. Schramm, D. J. Bamford, and C. B. Moore, Chem. Phys. Lett. **98**, 305 (1983); J. Kern, H. Schwahn, and B. Schramm, *ibid.* **154**, 292 (1989).
[14] C. R. Bowers and D. P. Weitekamp, Phys. Rev. Lett. **57**, 2645 (1986).
[15] D. Uy, M. Cordonnier, and T. Oka, Phys. Rev. Lett. **78**, 3844 (1997).
[16] T. Oka, in *Molecular Ions: Spectroscopy, Structure and Chemistry*, edited by T. A. Miller and V. E. Bondybey (North-Holland, Oxford, 1983).

[17] T. Oka, Rev. Mod. Phys. **64**, 1141 (1992).
[18] A. Dalgarno, Adv. At., Mol., Opt. Phys. **32**, 57 (1994).
[19] J. Tennyson, Rep. Prog. Phys. **57**, 421 (1995).
[20] I. R. McNab, in *Advances in Chemical Physics*, edited by I. Prigogine and S. A. Rice (Wiley, New York, 1995), Vol. LXXXIX, p. 1.
[21] T. R. Geballe and T. Oka, Nature (London) **384**, 334 (1996).
[22] B. J. McCall, T. R. Geballe, K. H. Hinkle, and T. Oka, Science **279**, 1910 (1998).
[23] J. Tennyson, S. Miller, and H. Schild, J. Chem. Soc., Faraday Trans. **89**, 2155 (1993).
[24] T. Oka, Philos. Trans. R. Soc. London, Ser. A **303**, 543 (1981).
[25] T. R. Geballe and T. Oka, Astrophys. J. **342**, 855 (1989).
[26] J. H. Black, E. F. van Dishoeck, S. P. Willner, and R. C. Woods, Astrophys. J. **358**, 459 (1990).
[27] K. F. Bonhoeffer and P. Harteck, Z. Phys. Chem. Abt. B **5**, 292 (1929).
[28] P. L. Chapovsky, L. N. Krasnoperov, V. N. Panfilov, and V. P. Strunin, Chem. Phys. **97**, 449 (1985); P. L. Chapovsky, Sov. Phys. JETP **70**, 895 (1990); Phys. Rev. A **43**, 3624 (1991); P. L. Chapovsky, D. Papousek, and J. Demaison, Chem. Phys. Lett. **209**, 305 (1993); A. E. Bakarev and P. L. Chapovsky, JETP Lett. **44**, 4 (1986); L. N. Krasnoperov, V. N. Panfilov, V. P. Strunin, and P. L. Chapovsky, *ibid.* **39**, 143 (1984).
[29] V. K. Konyukhov, A. M. Prokhorov, V. I. Tikhonov, and V. N. Faizulaev, JETP Lett. **43**, 85 (1986).
[30] H. G. Weber and M. Stock, Phys. Lett. A **50**, 343 (1974).
[31] R. A. Bernheim, C. He, and G. Alzetta, J. Chem. Phys. **92**, 5959 (1990); C. He and R. A. Bernheim, *ibid.* **95**, 8131 (1991).
[32] See, for instance, M. G. Bawendi, B. D. Rehfuss, and T. Oka, J. Chem. Phys. **93**, 6200 (1990).
[33] 1-Houdry, Division of Air Products and Chem. Inc. Philadelphia, PA (Apachi Nickel–Silica Catalyst No. 197-CP).
[34] M. W. Crofton, M.-F. Jagod, B. D. Rehfuss, W. A. Kreiner, and T. Oka, J. Chem. Phys. **88**, 666 (1988).
[35] C. M. Gabrys, D. Uy, M.-F. Jagod, T. Oka, and T. Amano, J. Phys. Chem. **99**, 15611 (1995).
[36] L. Kao, T. Oka, S. Miller, and J. Tennyson, Ap. J. Suppl. **77**, 317 (1991).
[37] T. Oka, Phys. Rev. Lett. **45**, 531 (1980).
[38] J. K. G. Watson, J. Mol. Spectrosc. **103**, 350 (1984).
[39] C. S. Gudeman and R. J. Saykally, Annu. Rev. Phys. Chem. **35**, 387 (1984).
[40] S. C. Foster, A. R. W. McKellar, and T. J. Sears, J. Chem. Phys. **81**, 578 (1984).
[41] J. U. White, J. Opt. Soc. Am. **32**, 285 (1942).
[42] J. H. Moore, C. Davis, and M. A. Coplan, *Building Scientific Apparatus* (Addison-Wesley, Reading, MA, 1983).
[43] A. von Engel, *Ionized Gases* (Oxford University Press, Oxford, 1965).
[44] J. L. Kieffer, At. Data **1**, 19 (1969).
[45] D. Rapp and P. Englander-Golden, J. Chem. Phys. **43**, 1464 (1965).
[46] M. Saporoschenko, Phys. Rev. **139**, A349 (1965); D. L. Albritton, T. M. Miller, D. W. Martin, and E. W. McDaniel, *ibid.* **171**, 94 (1968).
[47] V. G. Anicich and W. T. Huntress, Jr., Astrophys. J., Suppl. **62**, 553 (1986).
[48] A. B. Lees and P. K. Rol, J. Chem. Phys. **61**, 4444 (1974).
[49] K. R. Krenos, K. K. Lehmann, J. C. Tully, P. M. Hierl, and G. P. Smith, Chem. Phys. **16**, 109 (1976).
[50] J. E. Pollard, L. K. Johnson, D. A. Lichtin, and R. B. Cohen, J. Chem. Phys. **95**, 4877 (1991).
[51] N. G. Adams and D. Smith, Astrophys. J. **248**, 373 (1981).
[52] M. T. Leu, M. A. Biondi, and R. Johnsen, Phys. Rev. A **8**, 413 (1973).
[53] N. G. Adams, D. Smith, and E. Alge, J. Chem. Phys. **81**, 1778 (1984); N. G. Adams and D. Smith, in *IAU Symposium 120, Astrochemistry*, edited by M. S. Vardya and S. P. Tarafdar (Reidel, Dordrecht, 1987), pp. 1–18.
[54] H. Hus, F. B. Yousif, A. Sen, and J. B. A. Mitchell, Phys. Rev. A **38**, 658 (1988).
[55] T. Amano, J. Chem. Phys. **92**, 6492 (1990).
[56] A. Canosa, J. C. Gomet, B. R. Rowe, J. B. A. Mitchell, and J. L. Queffelec, J. Chem. Phys. **97**, 1028 (1992).
[57] M. Larsson, H. Danared, J. R. Mowat, P. Sigray, G. Sundström, L. Broström, A. Filevich, A. Källbeg, S. Mannervik, K. G. Rensfelt, and S. Datz, Phys. Rev. Lett. **70**, 430 (1993).
[58] A. Farkas, *Orthohydrogen, Parahydrogen, and Heavy Hydrogen* (Cambridge University Press, London, 1935).
[59] D. Uy, C. M. Gabrys, T. Oka, B. J. Cotterell, R. S. Stickland, and Ch. Jungen (unpublished).
[60] I. Langmuir, Phys. Rev. **26**, 585 (1925).
[61] D. Gerlich, J. Chem. Soc., Faraday Trans. **89**, 2199 (1993).
[62] M. Fehér, A. Rohrbacher, and J. P. Maier, Chem. Phys. **185**, 357 (1994).